Thin Solid Films 579 (2015) 68–74

Contents lists available at ScienceDirect

Thin Solid Films

journal homepage: www.elsevier.com/locate/tsf

Thin-film crystal growth of microcrystalline silicon using very-high-frequency hollow-electrode-enhanced glow plasma

Toshihiro Tabuchi [a,*], Yasumasa Toyoshima [a], Masayuki Takashiri [b,*]

[a] Research Division, Komatsu Ltd., 1200 Manda, Hiratsuka, Kanagawa 254-8567, Japan
[b] Department of Materials Science, Tokai University, 4-1-1 Kitakaname, Hiratsuka, Kanagawa 259-1292, Japan

ARTICLE INFO

Article history:
Received 12 August 2014
Received in revised form 13 February 2015
Accepted 16 February 2015
Available online 26 February 2015

Keywords:
Thin film
HEEPT
Microcrystalline silicon
VHF
Crystal growth

ABSTRACT

The thin-film crystal growth of hydrogenated microcrystalline silicon (μc-Si:H) on SiO_2 was investigated by using a very-high-frequency hollow-electrode-enhanced glow plasma system with an ultrahigh-vacuum reactor. The properties of the μc-Si:H thin films deposited with different flow rates of both mono-silane and hydrogen were characterized. We achieved fabrication of a μc-Si:H thin film with a growth rate of 4.0 nm/s, good photosensitivity, high crystallinity, and highly preferred crystal orientation along the <110> direction at a gas pressure of 80 Pa. To study the crystallographic structure in detail, cross-sectional transmission electron microscopy (TEM), limited-visual-field electron beam diffraction imaging, and high-resolution TEM were applied for the thin films deposited with the highest (4.0 nm/s) and lowest (0.25 nm/s) growth rates, respectively. The crystallographic images clearly show columnar growth of microcrystalline silicon in every region of the films, with a very thin transition layer less than 2 nm thick, suggesting direct growth from the substrate surface.

1. Introduction

Hydrogenated microcrystalline silicon (μc-Si:H) thin films are of great interest as the material for semiconductor devices such as thin-film transistors and solar cells because they could improve device performances by their higher electron mobility and/or preferable spectral response than those of hydrogenated amorphous silicon (a-Si:H) thin films [1–3]. In order to achieve high-quality μc-Si:H thin films with high-speed processing, many types of chemical vapor deposition (CVD) methods have been proposed, such as hot-wire CVD [4,5], radio-frequency (RF) and very-high-frequency (VHF) plasma-enhanced CVD (PECVD) [6–8], and surface wave-excited plasma CVD [9]. We previously proposed a plasma generation system called hollow-electrode-enhanced glow plasma transportation (HEEPT) [10–12], and we reported high-speed plasma CVD of high-quality μc-Si:H thin films by using a RF power source [10,13] and a VHF power source [14], and applying a magnetic field [15]. In our latest article, we also reported the effect of reducing oxygen concentration in the films using ultrahigh-vacuum system, in which the plasma was excited by RF power source [16]. Then, we achieved μc-Si:H thin films with preferential <110> crystal orientation retaining photosensitivity. It was also demonstrated that this system was able to deposit films of uniform thickness over a large area by contriving unique electrode [12].

In this work, we mainly focus on the preferential <110> crystal growth and microscopic structure of the μc-Si:H thin films for further improvement of the HEEPT fabrication technique at a low gas pressure. As it is considered that plasmas excited by higher frequency would be more effective for the preferential <110> crystal growth [7], VHF power source was applied for plasma generation instead of RF power source. The thin films, therefore, were deposited using an ultrahigh-vacuum HEEPT system, in which plasmas were excited by a VHF power source with a mixed gas of mono-silane (SiH_4) and hydrogen (H_2); the flow rate of these gases was varied as a parameter. The resulting thin films were investigated in terms of photoelectrical conductivity, crystallinity, crystal orientation, and atomic-level crystallographic structure. Finally, we discuss the mechanisms of crystal growth of the μc-Si:H thin films fabricated by the ultrahigh-vacuum VHF-HEEPT system.

2. Apparatus

The basic structure of the VHF-HEEPT system and the mechanism of plasma generation were described in our previous publications [11–13]. A schematic diagram of the VHF-HEEPT reactor is shown in Fig. 1. In brief, the VHF-HEEPT system consists of two spaces. One is a discharge space, having a VHF electrode (cathode electrode) made of aluminum and a counter electrode (anode electrode) also made of aluminum. The other is a deposition space, having a substrate holder with a heater. The VHF electrode has a showerhead structure with holes 3 mm in diameter for uniform distribution of the gases and a cave structure (the sub-discharge chamber) 5 mm in height. The holes and cave

* Corresponding authors.
E-mail addresses: toshihiro_tabuchi@komatsu.co.jp (T. Tabuchi), takashiri@tokai-u.jp (M. Takashiri).

http://dx.doi.org/10.1016/j.tsf.2015.02.050
0040-6090/

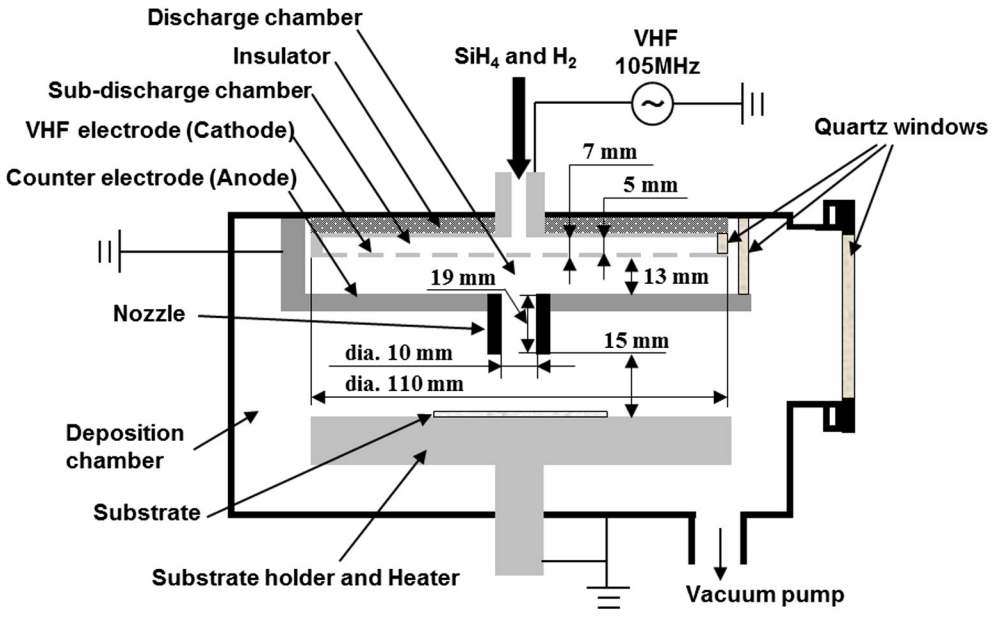

Fig. 1. Schematic of the ultrahigh-vacuum VHF-HEEPT reactor.

structure operate as a hollow-VHF-electrode discharge space. An orifice is prepared at the center of the counter electrode, and a straight aluminum tube (nozzle) is attached to the orifice. The total length of this nozzle including the thickness of the counter electrode is 19 mm and the internal diameter is 10 mm. The orifice and nozzle operate as a hollow-anode discharge space. The distance between the counter electrode and the VHF electrode is 13 mm, whereas the distance from the bottom end of the nozzle to the substrate holder is 15 mm. When process gases flow into the system and VHF power is applied to the VHF electrode, plasma is generated both in the discharge space and in the sub-discharge chamber, including in the holes of the cathode electrode. The plasma density is subsequently enhanced inside the nozzle, and the plasma then reaches the substrate located in the deposition space.

In order to reduce impurity concentration in the μc-Si:H thin films, we prepared an ultrahigh-vacuum HEEPT system [16]. The vacuum evacuation system consisted of a compound turbo-molecular pump and a dry vacuum pump. The vacuum-seal structure consisted of all-metal ultrahigh-vacuum gaskets, and the inner wall of the reactor, which was made of stainless-steel, was polished. The gas purification system was equipped in the hydrogen gas line. In addition, the reactor was baked using tape heaters at 200 °C. As a result, the background pressure and outgassing rate of the ultrahigh-vacuum HEEPT reactor decreased to 3.2×10^{-8} Pa and 2.7×10^{-6} Pa·L/s respectively.

3. Experimental details

The μc-Si:H thin films were deposited on silicon dioxide thin films on silicon wafers (SiO_2/Si) by using the ultrahigh-vacuum VHF-HEEPT system. The SiO_2 was 1.0 μm thick and was fabricated by using a thermal oxidation technique with hydrogen and oxygen in a quartz tube at 1100 °C. The silicon wafer was 525 μm thick, with a mirror-polished surface and a <100> orientation without an off angle. The Si wafers with SiO_2 were divided into pieces of 25 mm × 55 mm as a substrate. The flow rates of SiH_4 ([SiH_4]) and H_2 ([H_2]) varied from 1.5 to 6 sccm and from 30 to 80 sccm, respectively. The VHF power applied was 50 W. The substrate temperature, plasma excitation frequency, and gaseous pressure for film deposition were fixed at 300 °C, 105 MHz, and 80 Pa, respectively. The film thickness of this work was around 1.0 μm for the samples deposited by a hydrogen flow rate of 30 sccm, and around 3.0 μm for the others.

In order to compare the microscopic structure as a function of VHF power, an additional specimen was prepared at a lower VHF power. As is well known, we can obtain μc-Si:H thin films with better properties under lower plasma excitation power and lower gas flow rate; in other words, by depositing films slowly and carefully. The deposition conditions of the additional film were [SiH_4] and [H_2] of 1.5 and 40 sccm, respectively, and a VHF power of 20 W. Other conditions were the same as those used for the other samples (Table 1).

Regarding the film properties, the growth rate, impurity concentration, photoelectrical conductivity, crystallinity and crystal orientation were evaluated. The growth rate was calculated from the thickness of the area just below the nozzle. The radial profiles of the film thickness were measured at five points. One was that at the center of the film, while the others were ±3 mm, and ±5 mm from the center. The radial profiles of the film thickness were at most ±5% within the area mentioned above. The method and result are the same as our previous work [15]. We also confirmed that the radial profiles of the film were at most ±5% within 10 cm in diameter by applying spiral-shape orifice/nozzle as a hollow-counter-electrode. The impurity concentration of the film was analyzed using secondary ion mass spectrometry (SIMS). The primary ions applied to the SIMS measurement were Ce^+ of 14.5 keV for oxygen analysis (CAMECA IMS-4f) and O_2^+ of 8.0 keV for aluminum analysis (CAMECA IMS-6f). Dark conductivity and photoconductivity under an illumination of air mass 1.5 (AM1.5, 100 mW/cm^2: WACOM ELECTRIC WXS-156) were measured at room temperature using an ampere-meter/DC-voltage-source (Hewlett Packard HP-4140B). Crystallinity and residual stress were studied using Raman spectroscopy, which was measured by a microscopic Raman scattering system equipped with a 514.5 nm argon laser (RENISHAW SYS2000S). Residual stress was estimated by separating amorphous peak (480 cm^{-1}) and crystal peak (520 cm^{-1}) using curve fitting method. Crystal orientation and crystallinity were evaluated using X-ray diffraction patterns (XRD), which were obtained by an X-ray diffract meter system equipped with an X-ray tube of a rotating cupper target (JEOL JDX-8200). Fine crystallographic properties were examined using transmission electron microscopy (TEM), limited-visual-field electron beam diffraction imaging (EDI), and high-resolution TEM (HRTEM). TEM samples were prepared by argon ion